Earthquake Engineering, Tenth World Conference © 1992 Balkema, Rotterdam. ISBN 90 5410 060 5

Effectiveness of realized AMD response-control system

Y. Ikeda, K. Yamada & N. Koshika
Kobori Research Complex, Kajima Corporation, Japan

T. Kobori
Kyoto University & Kajima Corporation, Japan

ABSTRACT: A seismic-response-controlled structure was realized in Tokyo in August, 1989 for the first time in the world. Because the structure is a very slender ten-story office building, an Active Mass Driver (AMD) system has been installed to actively suppress vibrations under dynamic loadings such as earthquakes and winds. By February, 1992, the building had experienced more than ten earthquakes, during which measurements were taken of the responses of the structure and the control system. These measurements are simulated by a numerical analysis to represent the structure-control system interaction. By comparing the uncontrolled responses calculated without the AMD system, the effectiveness of the system is assessed.

1 INTRODUCTION

In recent years, the reduction of vibrations in structures has become an important issue, since social demand for improvement of safety and reliability has increased. This demand extends not only to safety against large seismic shocks of structures and vital equipment installed in them, but also to improvement in living comfort during vibrations caused by medium earthquakes. Seismic-response control is expected to mark a new approach to the design of anti-seismic structures.

In August, 1989, we realized a seismic-response-controlled structure for the first time in the world. Because the structure is a very slender ten-story office building, the Active Mass Driver (AMD) response-control system was installed on the roof level to actively suppress vibrations under nonstationary excitations such as earthquakes and winds. The AMD system consists of two auxiliary masses, two servo-actuators and control circuits. The actuators drive the masses and produce control forces to reduce vibrations in the transverse and torsional directions by means of an external energy supply, based on a feedback control algorithm. In designing the system, its dynamic characteristics were considered to represent the interaction between the structure and the control system.

From its completion in August, 1989 to February, 1992, the structure experienced more than ten earthquakes, during which the responses of the structure and the control system were recorded. These records are simulated by a numerical analysis which was proposed in the design. The comparison between the observations and the results of simulation indicates good correspondence, which verifies the validity of the employed analytical method and the modeling of the coupled structure-control system. Furthermore, the effectiveness of the AMD system is confirmed by comparing the controlled responses with the calculated uncontrolled responses.

2 ANALYTICAL METHOD

2.1 State equation of control system

A response-control system is composed of control circuits and mechanical equipment such as servo-actuator mechanisms. When the system is composed of plural elements connected in series, the dynamic characteristic can be expressed as the product of the transfer functions of all elements.

$$\bar{G}(s) = \bar{G}(i\omega) = \bar{G}_1(s)\bar{G}_2(s)\cdots\bar{G}_N(s) \qquad (1)$$

where s is $i\omega$, i is imaginary unity and ω is circular frequency. The transfer function represents the frequency-dependent time delay of the control system.

The Fourier transforms of the input $v(t)$ and the output $y(t)$, and the transfer function of the control system have the following relation.

$$F[y(t)] = \bar{G}(s)F[v(t)] \qquad (2)$$

where $F[\ ]$ is the Fourier transform.

The dynamic characteristic of the system is approximated by the rational function.

$$\bar{G}(s) = \frac{\bar{y}(s)}{\bar{v}(s)} = \frac{b_1 s^{n-1} + b_2 s^{n-2} + \cdots + b_n}{s^n + a_1 s^{n-1} + a_2 s^{n-2} + \cdots + a_n} \qquad (3)$$

where $\bar{v}(s) = F[v(t)]$ and $\bar{y}(s) = F[y(t)]$. Based on the initial condition $v(0) = y(0) = 0$, the Laplace inverse transform leads to the state equation and the output equation as follows.

$$\dot{x}(t) = Ex(t) + Fv(t) \qquad (4a)$$

$$y(t) = Hx(t) \qquad (4b)$$

$x(t)$ is defined as the state vector of the system.

Equations (4a) and (4b) are represented in discrete-time space by

$$x_L(k+1) = E_L x_L(k) + F_L v_L(k) \quad (5a)$$

$$y_L(k) = H_L x_L(k) \quad (5b)$$

where E_L, F_L and H_L are the transition matrices corresponding to E, F and H.

2.2 State equation of structure

When a structure with an AMD system is subjected to an arbitrary excitation, the matrix equation of motion can be expressed as

$$M\ddot{q}(t) + C\dot{q}(t) + Kq(t) = f(t) + Uu(t) \quad (6)$$

where M, C and K are the mass matrix, the damping matrix and the stiffness matrix, respectively; $q(t)$ is the displacement vector relative to the base; $u(t)$ is the control force vector; $f(t)$ is the external excitation force vector; and U is the location matrix of the controllers.

Equation of motion (6) can be rewritten in discrete-time space form as

$$x_B(k+1) = A_B x_B(k) + B_B u(k) + D_B f(k) \quad (7)$$

where x_B is a state vector of the structure.

2.3 State equation of structure-control system

The structure and the control system are coupled by

$$u(k) = L y_L(k) \quad (8a)$$

$$v_L(k) = H x_B(k) \quad (8b)$$

where the matrix L represents the relation between the output of the system y_L and the control force u, and the matrix H represents the relation between the response of the structure x_B and the input of the system v_L. When Equations (5a), (5b) and (7) are coupled under the relations (8a) and (8b), the extended state and output equations of the structure-control system can be obtained as follows.

$$\begin{bmatrix} x_B(k+1) \\ x_L(k+1) \end{bmatrix} = \begin{bmatrix} A_B & 0 \\ F_L H & E_L \end{bmatrix} \begin{bmatrix} x_B(k) \\ x_L(k) \end{bmatrix} + \begin{bmatrix} B_B L \\ 0 \end{bmatrix} y_L(k) + \begin{bmatrix} D_B \\ 0 \end{bmatrix} f(k) \quad (9a)$$

$$y_L(k) = H_L x_L(k) \quad (9b)$$

In addition, if it is permissible to use the one-step-delay structural response as the input of the system, the responses can be calculated from Eqs.(10a) to (10e) instead of from Eqs.(9a) and (9b). In this analysis, calculations are repeated step by step.

AMD system

$$v_L(k) = H x_B(k-1) \quad (10a)$$

$$x_L(k+1) = E_L x_L(k) + F_L v_L(k) \quad (10b)$$

$$y_L(k) = H_L x_L(k) \quad (10c)$$

Structure

$$u(k) = L y_L(k) \quad (10d)$$

$$x_B(k+1) = A_B x_B(k) + B_B u(k) + D_B f(k) \quad (10e)$$

The nonlinearity of the system can be considered, since the method is proposed in the time domain.

3 SIMULATION MODEL

3.1 Objective structure

A ten-story office building, shown in Fig. 1, was chosen for the control. Its height-to-width ratio is 9.5, indicating that it is very slender. It is constructed of rigidly connected steel frames of four box columns and H-shaped beams. The total weight of the building for simulation is about 270 tons. As shown in the typical floor plan, the weight distribution of the floors is eccentric in the longitudinal direction. Because of its slenderness and weight eccentricity, the transverse and torsional directions were selected for the control. Two auxiliary masses are suspended from the frames on the 11th floor and each mass is expected to suppress the response in one direction. The weights are 4.2 tons for auxiliary mass No.1 (AMD1) and 1.2 tons for mass No.2 (AMD2)

Not only the main frames but also secondary members such as external walls and partitions are considered in the modeling. Under the rigid floor assumption, three degrees of freedom, in the longitudinal, transverse and torsional directions, are represented at the mass center of each floor. The model is reduced to a three-dimensional bending and shear beam model with 36 degrees of freedom and is fixed at the first floor level where the seismic motion is input. Internal viscous damping is assumed with a ratio of 0.01 at the first natural period of the building.

The weight, stiffness and mass center are estimated to simulate the natural periods and vibration modes obtained from the vibration tests. The natural periods and participation factors of the building model are shown in Table 1. The first mode is dominant in the transverse direction, and the third mode in the torsional direction. Higher modes, from fourth to sixth, are 2nd modes in each direction.

Table 1 Natural periods and participation factors of building model for simulation

Mode	Natural period(s)	Participation factor Trans.	Longi.	Note
1	0.929	1.60	0.01	Trans. 1st
2	0.645	0.03	1.34	Longi. 1st*
3	0.537	0.29	0.13	Tor. 1st
4	0.274	0.62	0.00	Trans. 2nd
5	0.215	0.02	0.53	Longi. 2nd*
6	0.174	0.39	0.07	Tor. 2nd
7	0.165	0.01	0.06	Tor. 3rd
8	0.135	0.16	0.10	Trans. 3rd
9	0.124	0.10	0.21	Longi. 3rd*

* The longitudinal direction is uncontrolled

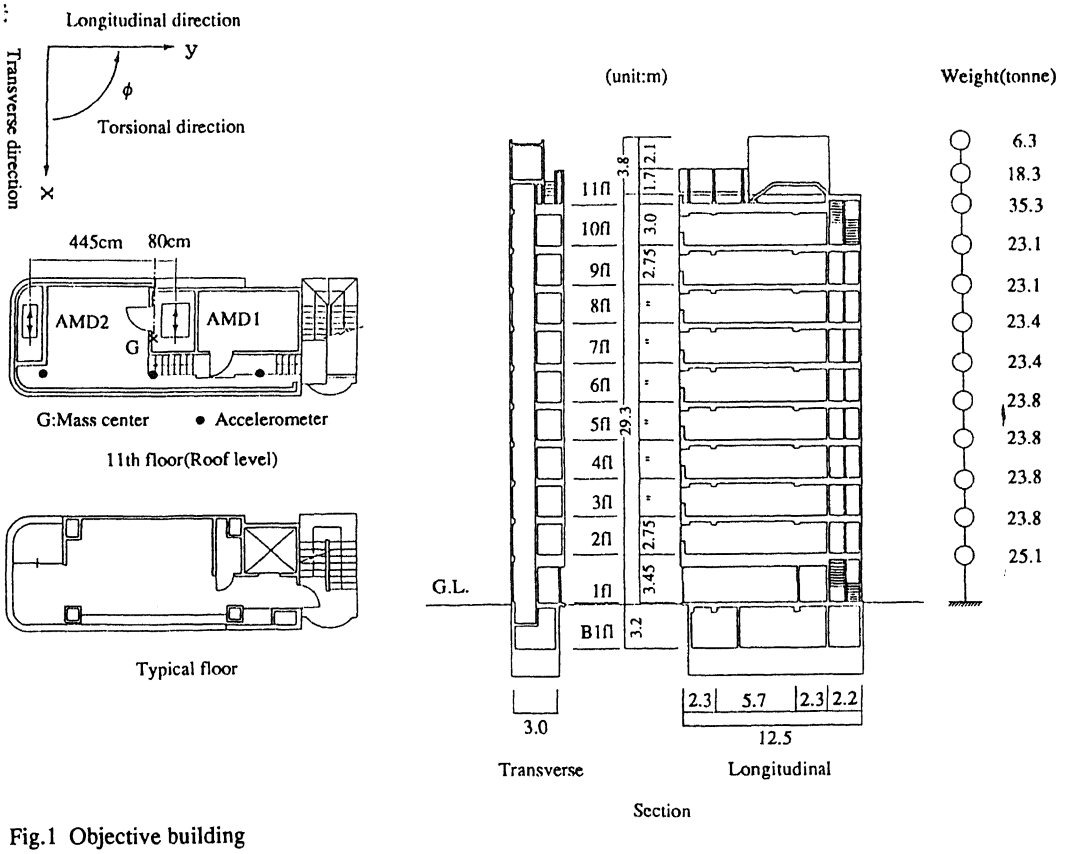

Fig.1 Objective building

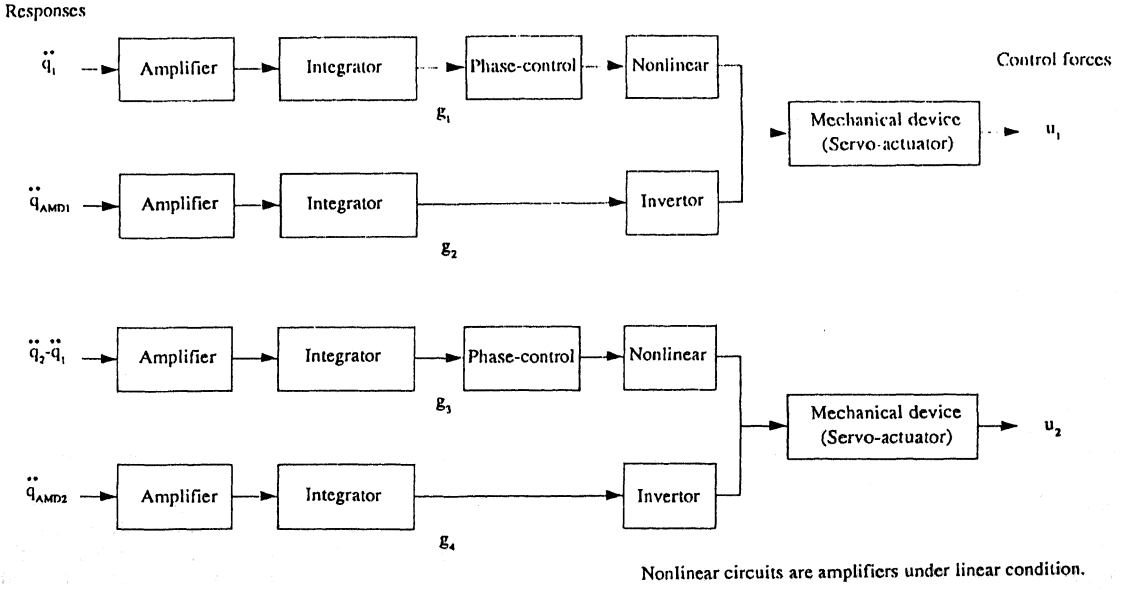

Fig.2 Control system

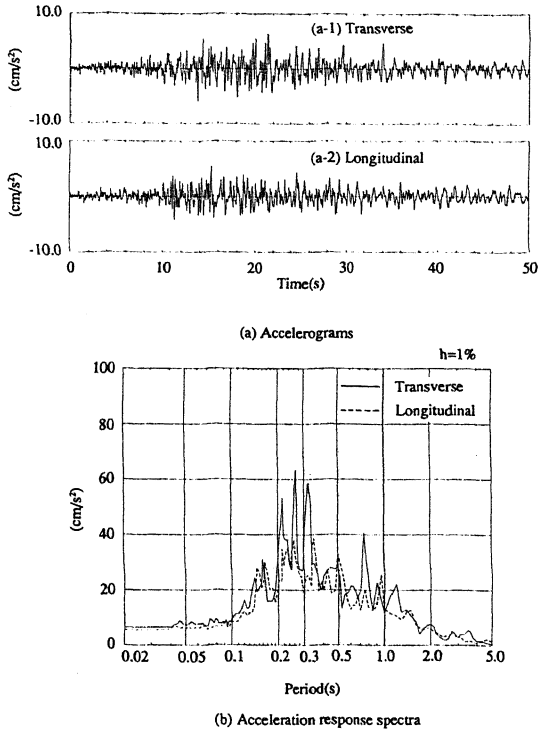

Fig.3 Earthquake acceleration at B1 floor on June 1, 1990

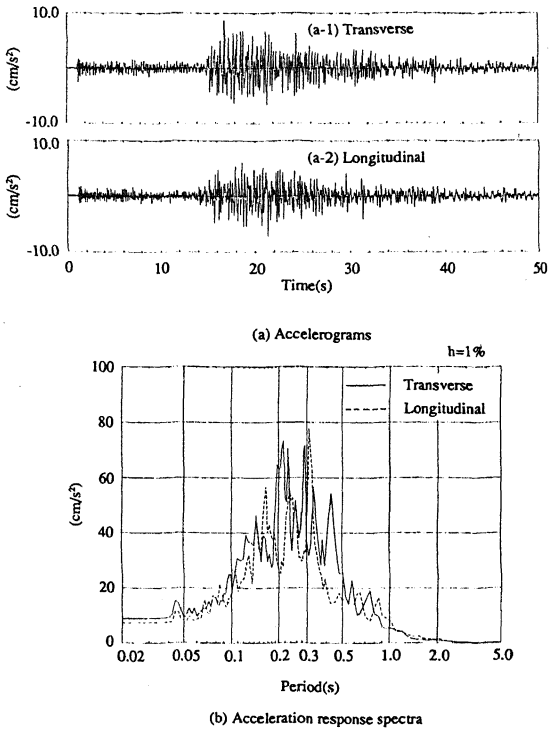

Fig.4 Earthquake acceleration at B1 floor on June 5, 1990

3.2 Control system

The AMD system consists of two auxiliary masses, two servo-actuators and control circuits. The servo-actuators drive the auxiliary masses to generate control forces, based on the feedback-control algorithm (11a) for AMD1 and the algorithm (11b) for AMD2.

$$u_1 = g_1\ddot{q}_1 + g_2\ddot{q}_{AMD1} \tag{11a}$$

$$u_2 = g_3(\ddot{q}_2 - \ddot{q}_1) + g_4\ddot{q}_{AMD2} \tag{11b}$$

where u_1 and u_2 are the control forces; $\ddot{q}_1$ and $\ddot{q}_2$ are the transverse accelerations at the locations of auxiliary masses relative to the base; $\ddot{q}_{AMD1}$ and $\ddot{q}_{AMD2}$ are the relative acceleration of masses; and g_1 , g_2 , g_3 and g_4 are feedback gain, depending on the frequency of input signals.

The control system is arranged as shown in Fig.2. The rational function of each element is identified from the analyses and experiments. The nonlinear elements are necessary to restrict the maximum control forces under large-scale excitations.

4 OBSERVATION RECORD

The input earthquakes for simulation were recorded at the first basement (B1) floor of the building on June 1 and June 5, 1990. The data of these earthquakes and the maximum values of acceleration at the B1 floor are shown in Table 2. The accelerograms and the response acceleration spectra are shown in Figs.3 and 4.

Table 2 Observed earthquakes

Data: June 1, 1990 Epicenter : Off East Cost of Chiba, Japan Magnitude : 6.0 Focal depth : 59 km Epicenter distance: 80 km Maximum acceleration at B1 floor : 6.4 cm/s² (Trans.), 5.4 cm/s² (Longi.)
Data: June 5, 1990 Epicenter : Middle of Kanagawa, Japan Magnitude : 5.3 Focal depth : 120 km Epicenter distance : 50 km Maximum acceleration at B1 floor : 8.8 cm/s² (Trans.), 7.2 cm/s² (Longi.)

On conducting the simulation analyses, the earthquakes are input at ground level, since only the above-ground portion of the building is modeled. Two earthquakes observed at the B1 floor in the transverse and longitudinal directions are regarded as input waves and input to the three-dimensional analytical model.

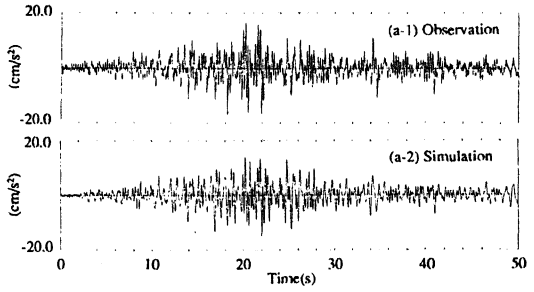

(a) Transverse accelerogram at 11th floor

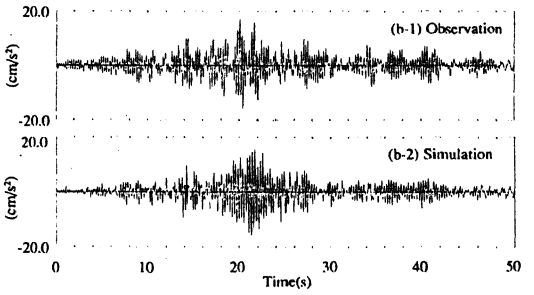

(b) Transverse accelerogram at 6th floor

Fig.5 Observed responses at 11th and 6th floors under earthquake on June 1, 1990, showing comparison with simulation

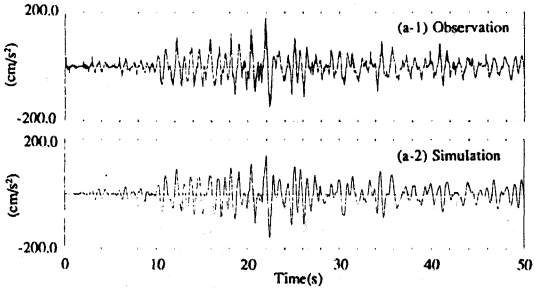

(a) Accelerogram of auxiliary mass No.1

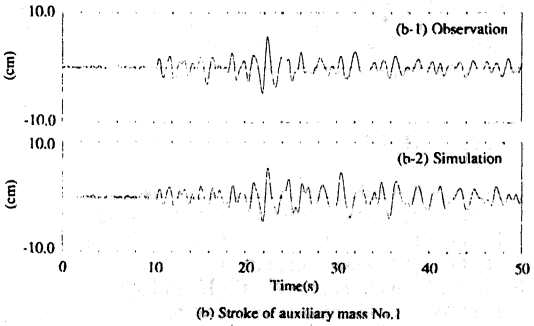

(b) Stroke of auxiliary mass No.1

Fig.6 Observed motion of AMD1 under earthquake on June 1, 1990, showing comparison with simulation

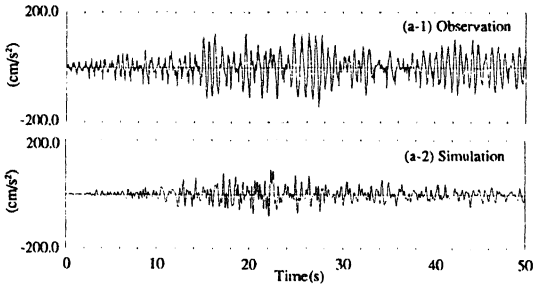

(a) Accelerogram of auxiliary mass No.2

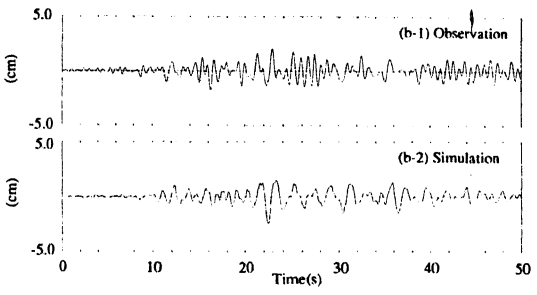

(b) Stroke of auxiliary mass No.2

Fig.7 Observed motion of AMD2 under earthquake on June 1, 1990, showing comparison with simulation

5 SIMULATION ANALYSIS

5.1 Simulation for observation

The observed records for June 1, 1990 are shown in Figs.5 to 7, compared with the results of simulation analyses using the method described in Section 2 and the model in Section 3. The transverse accelerations at the 11th and 6th floors are shown in Fig.5; the motion of AMD1 in Fig.6 and the motion of AMD2 in Fig.7.

The simulation at the 11th floor shows very good agreement with the observation, in magnitude, the transition of periods and the time at which the maximum response occurs. The simulation at the 6th floor approximates the observation. The simulation for AMD1 corresponds to the record in both the stroke and the acceleration. On the other hand, the simulation for AMD2, which acts to control the torsional vibration, does not agree well. This disagreement is due to the difficulty in modeling the torsional dynamic characteristics of the structure, which are determined from weight and stiffness distributions at every floor. It is confirmed that the dynamic characteristics of the AMD system can be identified precisely and the observation in the transverse direction can be simulated well. The same tendency between simulation and observation is recognized under the earthquakes occurring on June 5.

The simulation for observation substantially verifies the validity of the employed analytical method and the modeling of the structure-AMD control system, and the control effect can be estimated using the same method and model in Section 5.2.

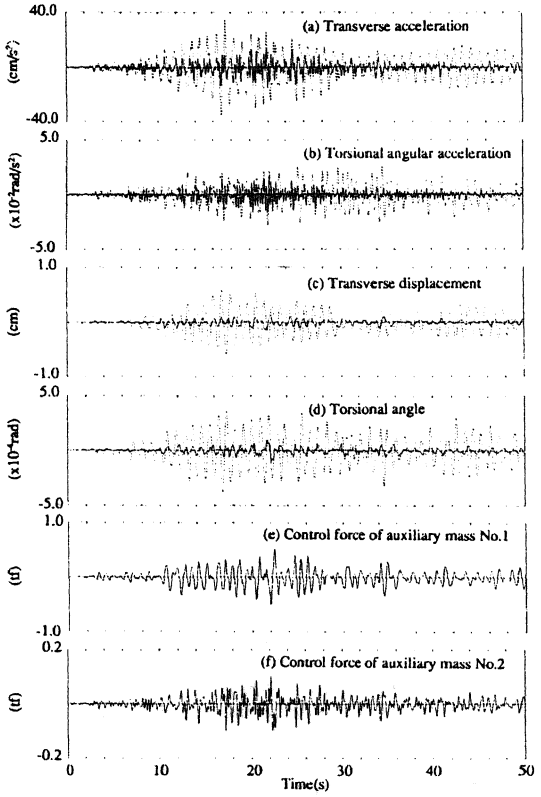

Fig.8 Control effect at 11th floor and control forces under earthquake on June 1, 1990
(Solid lines: controlled, Dashed lines: uncontrolled)

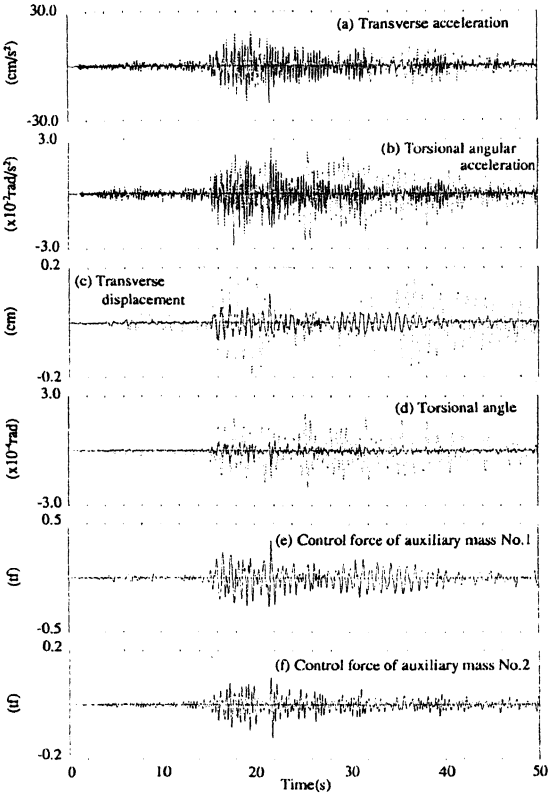

Fig.9 Control effect at 11th floor and control forces under earthquake on June 5, 1990
(Solid lines: controlled, Dashed lines: uncontrolled)

5.2 Estimation of control effect

The control effect on June 1 is estimated as shown in Fig.8 and the effect on June 5 as shown in Fig.9. The controlled responses are also calculated employing the analytical model.

The control target in the design was to reduce the maximum accelerations and displacements in the transverse and torsional directions at the top floor by 1/3 to 1/2 under medium earthquakes. Under the earthquake on June 1, the control effect is very high in both accelerations and displacements, and the system could achieve the control target. Under the earthquake on June 5, the control effect is very high in displacements, but low in accelerations.

The difference in the control effects depends on the interaction between the structure, the control system and the input excitation. The proposed system reduces vibrations easily under earthquake excitations that have power at the dominant transverse and torsional natural periods, because the control forces are applied on the floor nearest the anti-node of the dominant modes. The comparison of the response acceleration spectra at the B1 floor shows that the earthquake on June 1 has more power than the one on June 5 at the dominant transverse period.

6 CONCLUSIONS

The seismic-response-controlled structure with the Active Mass Driver (AMD) system was realized, and the responses of both the structure and the system were recorded under earthquakes. The observation was simulated by the analytical method that represents the structure-control system interaction. The simulation verified the proposed method, the analytical model and the control effectiveness. It was assessed that the control effect depends on the dynamic characteristics of input earthquakes.

REFERENCES

Kobori,T., Koshika,N., Yamada,K., & Ikeda,Y. 1991. Seismic-response-controlled structure with Active Mass Driver system. Part 1:Design & Part 2:verification. Earthquake eng. struct. dyn. 20: 133-166.

Ikeda,Y., Yamada,K., Sasaki,K., Koshika,N. and Kobori,T. 1991. Effectiveness of realized seismic-response-controlled structure with Active Mass Driver System. Journal of structural and construction engineering (Transaction of AIJ). 420: 133-141.